Bright Ideas in Fiber Optics

Measurement & Test Report

LAPPD #29

Fabrication Date: 3/21/2018

INCOM, INC.
294 Southbridge Road
Charlton, MA 01507-5238

Tel: (508) 909-2200
Fax: (508) 909-2323

LAPPD #29 General Features and Parameters:

Feature	Parameter
Photodetector Material	Borosilicate Glass
Window Material	Fused Silica Glass
Photocathode Material	Multi-Alkali (K_2NaSb)
Spectral Response (nm)	160-850
Wavelength – Maximum Sensitivity (nm)	<= 365 nm
Photodetector Active Area Dimensions	195mm X 195mm
• Minimum Effective Area	34,989 mm^2 **[(195*195)- {(2*265*6) – (6x6)}]**
• Active fraction with Edge Frame X-Spacers	92% **[(195*195)- {(2*265*6) – (6x6)}] / (195 * 195)**
Anode Data Strip Configuration	28 silver strips, Width = 5.2 mm, gap 1.7 mm, nominal 50 Ω Impedance
Voltage Distribution	5 taps for independent control of voltage to the photocathode and entry and exit of MCP

LAPPD # 29 Operational Ratings

Parameter	Rating
Supply voltage Photocathode — Anodes (Volts)	Typical: • 30V between MCP and photocathode • 850 V/MCP • 200 V between MCPs & MCP and anode • Photocathode voltage is -2130 V Maximum: Photocathode voltage at -2900 V
Operating ambient temperature °C	TBD (nominal room temperature)
Storage temperature °C	-12 to 50 (Avoid indium seal melt)

LAPPD Package / Housing Characteristics

Parameter	Rating
Photodetector Physical Dimensions (L X W X Thickness, mm)	230 x 220 x 22
Photodetector Mounting Case	ULTEM or equivalent dielectric polymer
Photodetector Mounting Case Dimensions	243 mm X 274 mm X 25.2 mm
Connectivity	Passive PC Interface Board , (300 mm X 264 mm X 1.6mm)
Overall Footprint, with Mounting Case & PC Interface Board	300 mm X 274 mm X 26.8 mm
Shipping Container	Pelican Case + Cardboard Box + G-force indicators

LAPPD #29 Microchannel Plate (MCP) Features & Performance

MCPs	Two Arranged in a Chevron Pair
Dimensions	203 mm x 203 mm X 1.2 mm
MCP Substrate	Incom C5 and C14 Glass
Capillary Pore Diameter (µm) Center to Center Pitch (µm)	20 25
Channel Length / diameter Substrate Thickness (mm)	60:1 1.2
Bias Angle	13
Capillary Open Area Ratio	≥64%
Resistive and Emissive Coatings	Chem 1, Applied via Atomic Layer Deposition (ALD)
Secondary Emission (SEE) Layer Material	MgO
Electrode Penetration – Input & Output (Pore Diameter)	1
MCP ID (Entry / Exit)	C00101-049 / C00113-028
MCP Chevron Pair Gain (@ Measurement & Test)	N/A
MCP resistance (Entry/Exit)	3.8 / 1.4 Mohms at 850 V Onlinemetadata_20180515_Spellman.xlsx
Dark Counts	6.5 kHz/cm^2 at a threshold of 8E5 gain (134 fC), 850 V/MCP, 30 V on photocathode (OnlineMetaData_20180515 Spellman with plots.xlsx)
Max Voltage	850/850 v/MCP recommended (entry/exit), -2900 volts at the photocathode maximum.

LAPPD #29 Operating Performance

Parameter	Performance
Photocathode Quantum efficiency (QE @ 365 nm) =	Mean QE (@365 nm) =6.75%,
Photocathode QE Spatial Variability (σ)	4.6%
Tile Dark Count rate	0.45 Cts/S cm^2 at a threshold of 2.5E5 gain (40.5 fC)(Onlinemetadata_20180130_Spellman.xlsx, 0V on P/C, 875 V/MCP
LAPPD Gain @ 850 Volts =	5.6 X10^6 @ 850/850 V (entry/exit), with variation = σ ≤ 50% mean
Dark / Background Rate @ gains ≥ 0.1 PE	
Time response (Min, Typical, Max) PS	TBD

Introduction

Functional tests were performed on LAPPD 29 in a dark box that was fitted with a UV light source and signal acquisition hardware. Some tests were performed at the second LAPPD Workshop in May 2019 at Incom. A summary of the results is shown below. The measurements include:

1. **Gain**
    - Gain vs. MCP voltage
    - Gain vs. photocathode voltage
    - Gain vs. repetition rate
2. **Dark rates** vs. MCP and photocathode voltage
3. **Timing and Position**
    - Position along a strip, inferred from relative pulse arrival times at each end
    - Position across strips from centroiding
4. **Transit Time Variation**
5. **Photocathode QE spectrum and map**
6. **MCP** resistance vs. voltage

Gain vs. MCP voltage

Gain was measured as a function of MCP voltage, using PSI DRS4 waveform samplers. MCP pulses were produced by directing a 405 nm Edinburgh Instruments 60 pS UV pulsed laser to a selected point on the LAPPD window. The laser was triggered externally at 1.8 kHz.

A neutral density filter (NE540B from Thorlabs) was used on the laser to reduce the intensity to the single photon level. The LAPPD responded to 5 out of every 20 laser pulses.

The gain results are shown in Figure 1 as a function of MCP voltage. The LAPPD gain for essentially single photoelectrons is as high a 1.1E7 at 900 volts/MCP. The pulse height distributions are also shown in Figure 2, for 30 V on the photocathode and 200 volts on the photocathode. The distributions are similar, but shifted to high gain at the higher photocathode voltage. This is consistent with the expected increase in the number of secondary electrons from the MgO film as incident electron energy rises (Jokela, 2012).

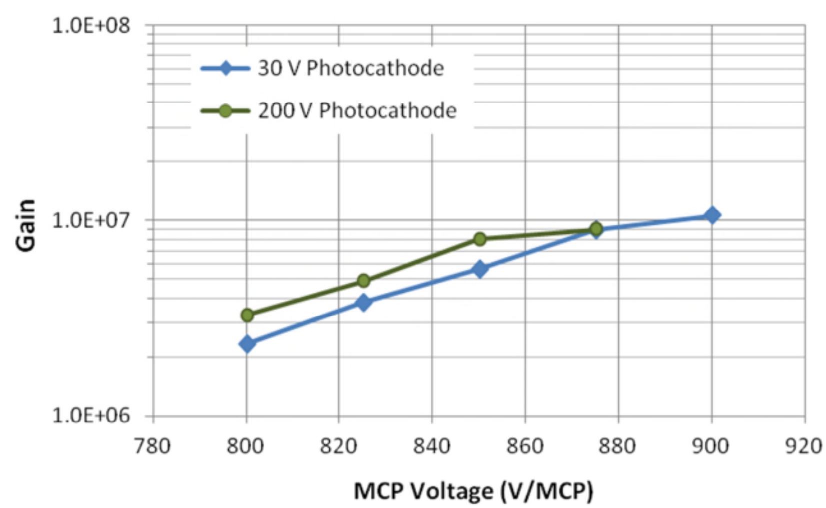

Figure 1: Gain is shown vs. MCP voltage, as measured with PSI DRS4 waveform samplers.

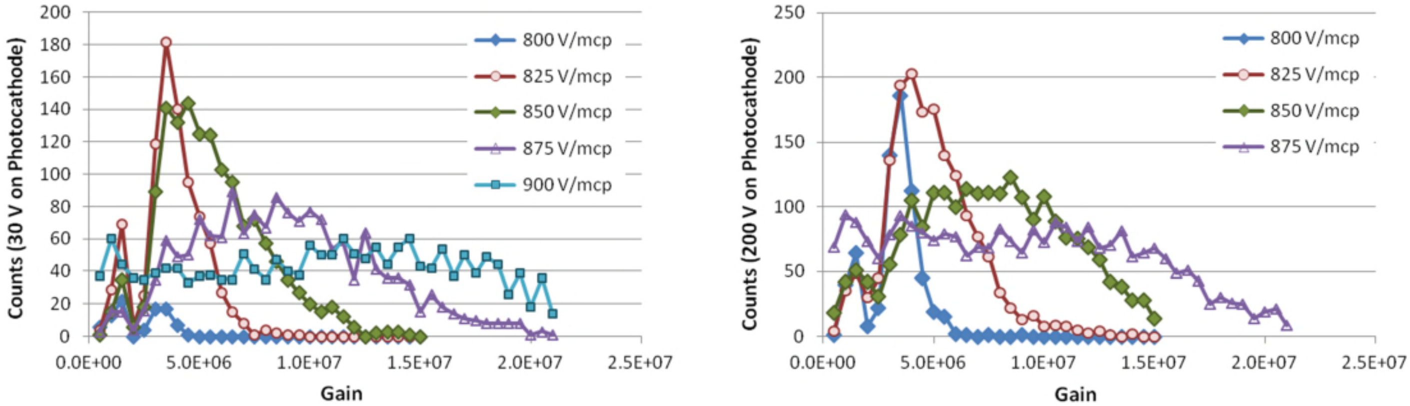

Figure 2: Gain is shown as a function of two photocathode voltages, at selected MCP voltages.

Gain vs. repetition rate

When a microchannel produces a charge pulse, it needs time to recharge. Otherwise, subsequent pulses will be smaller than the first. The microchannel plates are suitable for high rate conditions because the channels are nearly independent of each other, and unless the same one is struck twice, they will have time to recover.

The reduction of gain as a function of rate was tested by applying the 405 nm laser to a spot on the LAPPD window, of about 1 mm in diameter. The repetition rate was changed, and the corresponding gain was measured. Figure 3 shows the result, in which the gain declines by a factor of approximately two as the rate is increased from 9 kHz/3mm^2 to 400 kHz/3mm^2. Both LAPPD 22 and 25 are shown in Figure 3. LAPPD 29 has MCPs with relatively low resistance, about 1-4 Mohms, so the MCPs can recharge as effectively as possible.

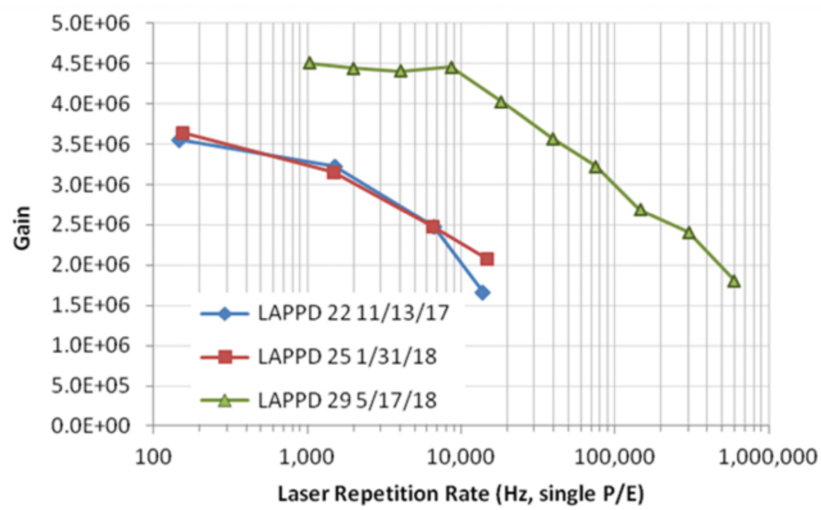

Figure 3: Gain is shown vs. laser repetition rate for single photoelectrons.
OnlineMetadata_20170810_Spellman with plots.xlsx

The gain in Figure 3 is shown as a function of laser repetition rate. All three LAPPDs responded with approximately the same frequency to the laser, or 2-4 responses out of 10 laser pulses. Figure 4 shows the gain as a function of observed pulse rate, rather than the laser trigger rate. At this rate, the gain dropped to half as the observed rate increased from 40 Hz/3mm^2 to ~15 kHz/3mm^2. This rate is somewhat thresholddependent, so at higher rates, some pulses fall below threshold. The pulse distributions as a function of laser trigger rate are shown in Figure 5. At higher rates, the pulse height distributions shift to the left, corresponding to reduced gain.

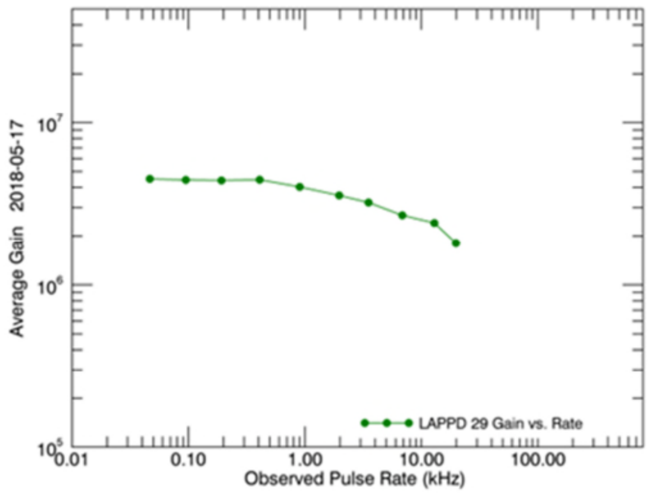

Figure 4: Gain is shown vs. observed pulse rate for single photoelectrons.

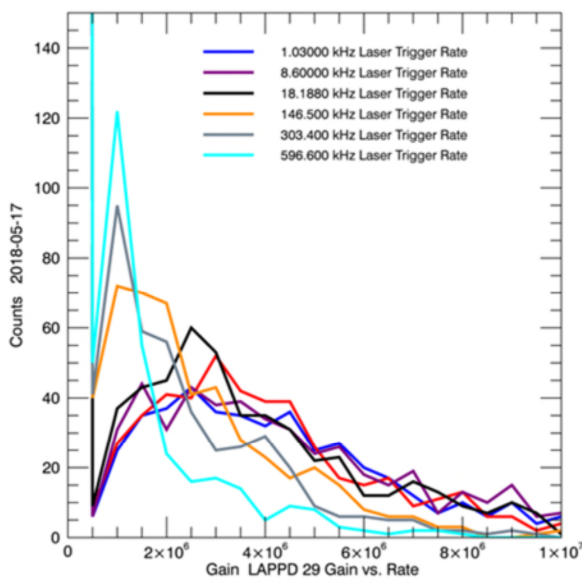

Figure 5: The pulse distributions are shown as a function of laser trigger rate.

Dark rates vs. MCP and photocathode voltage

Dark rates are shown in Figure 6 as a function of MCP voltage and photocathode voltage. The higher photocathode voltages tend to increase the gain, but they also increase the dark rates. These rates were acquired from a single strip. Also shown in Figure 6 are dark rates as a function of the time delay from setting a photocathode voltage until the dark rate was measured. A slow decline was observed, by approximately a factor of two in 9 minutes.

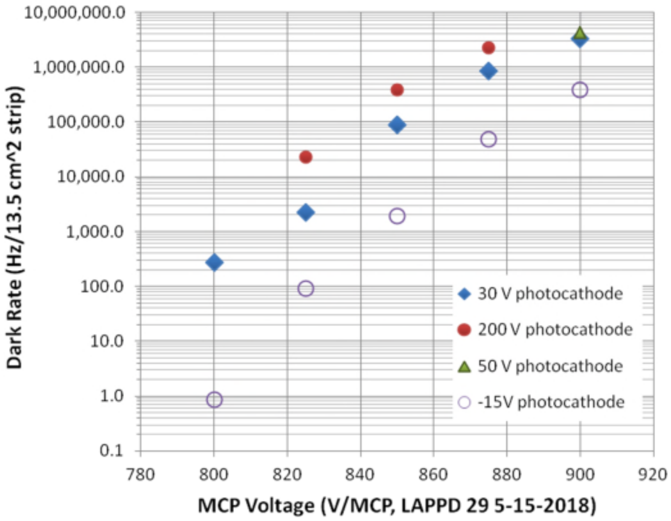

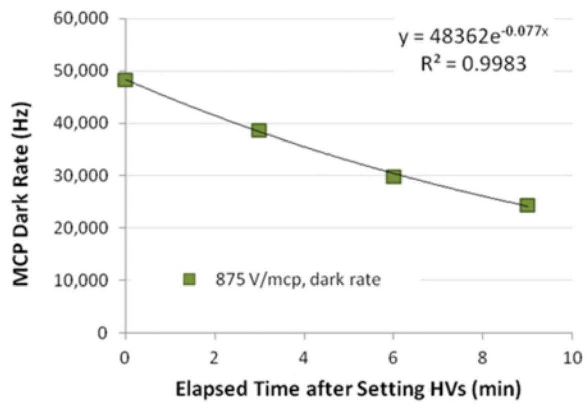

Figure 6: Left - Dark rates are shown as a function of MCP voltage, and of photocathode voltage. Right – Dark rates are shown as a function of time after setting the voltages. (OnlineMetadata_20180515_Spellman.xlsx)

Position along a Strip

Position may be measured with the LAPPD stripline anode in two ways. Along a strip, the position of the charge pulse may be inferred by measuring the relative time of arrival of pulses at each end of the strip, as the charge deposited by the MCP makes its way to ground at both ends. The time needed for a pulse to travel the entire strip is combined with the difference in arrival time at both ends, and cable offsets are subtracted to calculate the position of charge deposition. This process is shown schematically in Figure 7, right.

A scan of the 405 nm laser along a strip was observed using a pair of DRS4 waveform samplers, and the variation in relative timing therefore measured.

The results of the position scan are shown on the left side of Figure 7. There is a small discontinuity at +10 and +20 mm. These can occur where the laser hits an area of the photocathode with an X-spacer underneath. When the laser light is completely obscured this way, the observed position is the average of dark pulses, which tends to be near the center.

The position resolution along a strip is determined by the arrival time measurement of the pulses at the ends. The distribution in time differences observed at the ends of one strip in shown in Figure 8. The position resolution is 2.2 mm at the laser position of 50 mm. The sigma of this distribution is shown as a function of position in Figure 8 (right). The large variation at the position +10 mm is the result of a laser spot landing on an X-spacer, so that only dark pulses contribute to the position measurement.

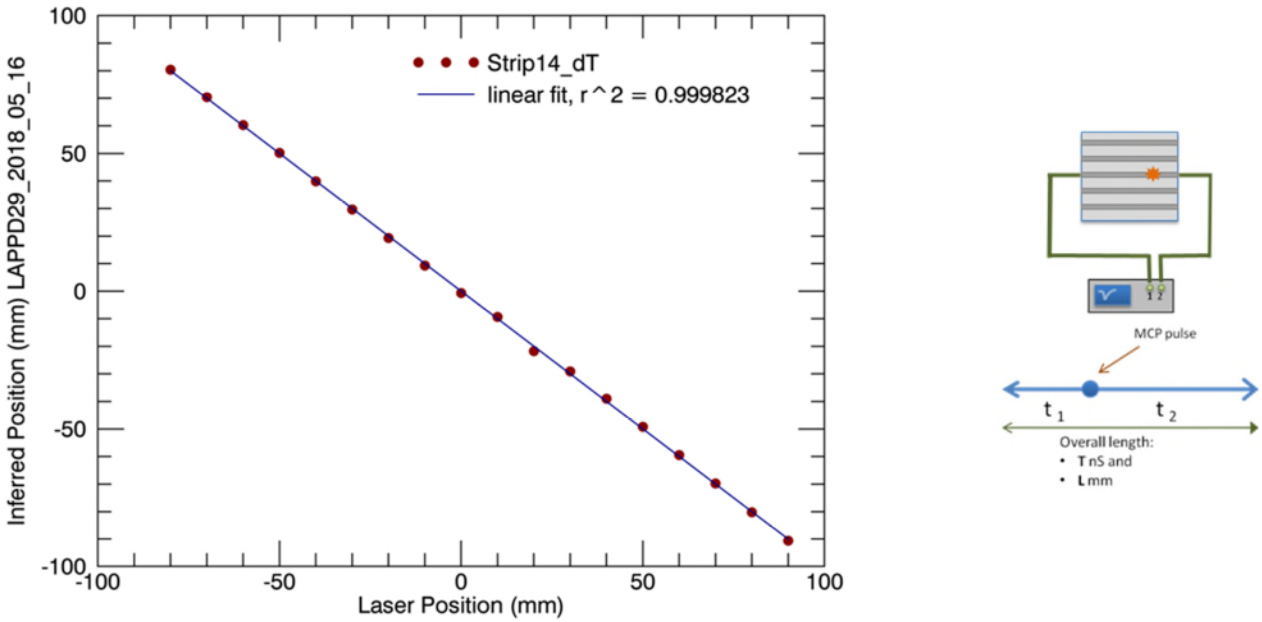

Figure 7: Position is inferred from average pulse arrival times at each end of a strip, and plotted against the known laser position. There is a 2.2 mm uncertainty in position. Right: pulses are observed at the left and right ends of a strip. Their relative arrival time leads to position of the charge deposition along the strip.

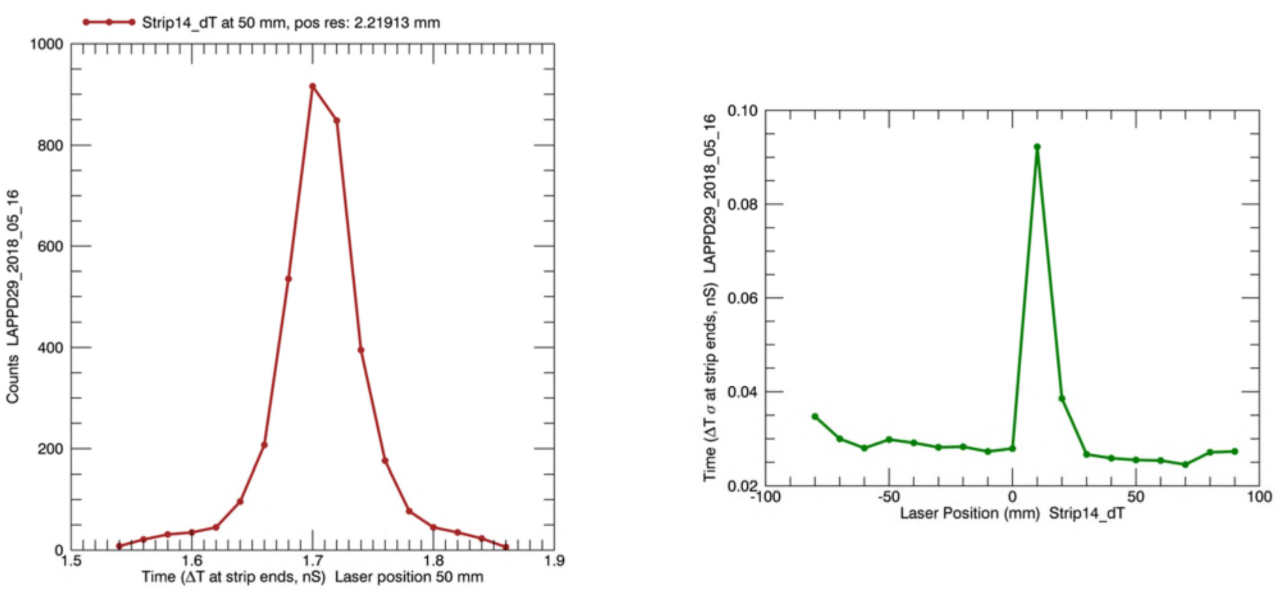

Figure 8: Left - The time distribution is shown for pulses arriving at the ends of a strip, from a laser pulse at the position 50 mm. Right – the width of the time distribution is shown as a function of position along the strip. Note the discontinuity at +10 and +20 mm.

Position Across Strips

Position may be measured across strips as well. In this case, the centroid of five adjacent strip signals may be calculated, resulting in the position to a better resolution than the strip pitch itself. Instead of using timing, the distribution of charge among the adjacent strips is used to calculate position. The relative charge deposition on 5 adjacent strips is shown in Figure 9, as the laser was moved across strips in 1 mm steps. A potential difference of 500 volts was applied between the exit MCP and the anode. This creates the tendency to localize the charge deposition on single strips. A tradeoff is expected between position resolution and timing resolution as a function of this voltage, where timing should improve with a large voltage, at the expense of position resolution.

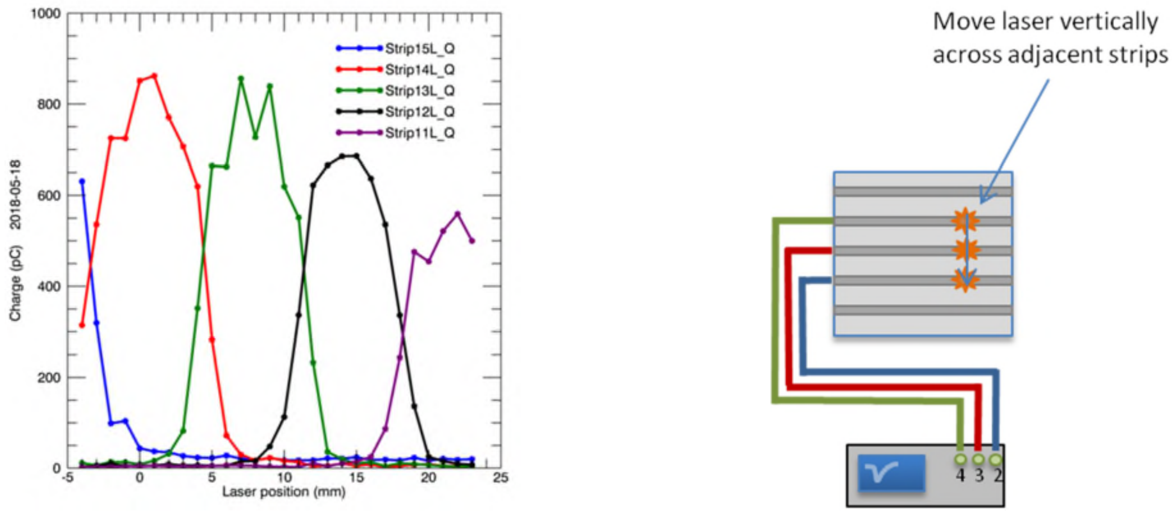

Figure 9: Left - The relative charge distribution among 5 adjacent strips is shown as a function of laser position. Right – a sketch of the laser movement is shown.

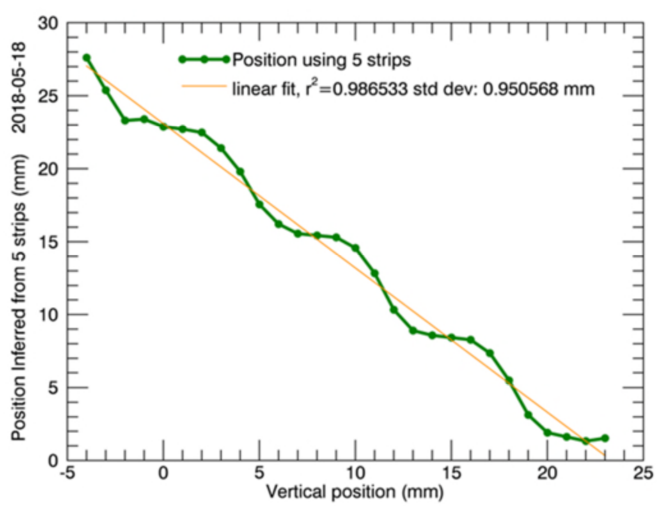

Figure 10: Position as inferred from charge distributions on adjacent strips is shown as a function of laser position.

The inferred laser position is shown in Figure 10, using the relative charge deposition on each of 5 adjacent strips. The position resolution is expressed as the deviation from linearity, and is 0.95 mm. A linear fit is superimposed. A future measurement will repeat this cross-strip scan at a lower voltage between the MCP and anode, and compare position and timing resolution at the two voltages.

Transit Time Variation

The variation between initiation of a photoelectron and the corresponding pulse arrival at the end of a single strip is of interest for timing applications. A fast photodiode was used to directly monitor the 405 nm laser pulse. The time difference between the monitor pulse and the corresponding pulse from a single strip was measured. The variation in this time is the transit time variation of the LAPPD. Variations may come from phenomena such as the depth to which the photoelectron advances into the microchannel before striking the walls of the channel. Additional variations arise from electronic noise superimposed on the strip measurement. Hence, the quality of the measurement is somewhat environment-dependent, and the result here may not be the best achievable with the LAPPD.

The 405 nm laser that is used for the LAPPD tests has a 60 pS firing window. The intensity is reduced by neutral density filters to produce single photoelectrons. Therefore, the laser photon that produces the single electron may arrive at any time within the 60 pS window. The transit time distribution is shown in Figure 11. The standard deviation of the distribution is 96 pS. If the variation of the laser photon has a standard deviation of 60 pS, then the LAPPD transit time variation may be extracted as a sum of squared variations as 75 pS.

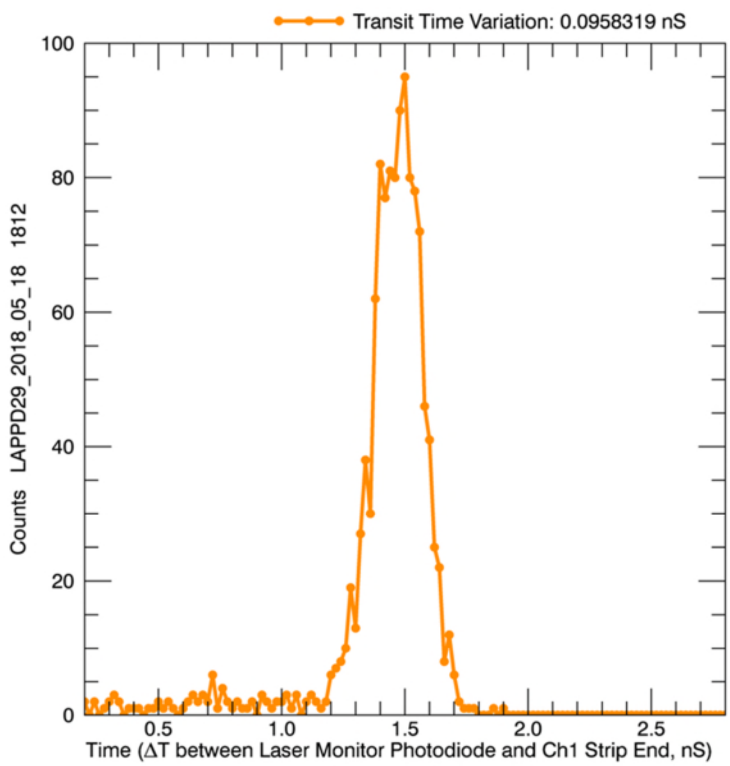

Figure 11: The transit time variation is shown. This is the time difference between the observed laser firing and the arrival of a corresponding pulse at the end of an anode strip.

Photocathode QE spectrum and map

The quantum efficiency of the photocathode was measured across the LAPPD window by scanning a 365 nm UV LED in an XY pattern of 3 mm steps. The illumination on the window had a circular pattern with a ~2.5 mm diameter. The intensity of the input light was measured with a Thorlabs SM1PD2A photodiode, and a Keithley 6485 picoammeter. The photocurrent was collected by connecting both sides of the entry MCP to a Keithley

2400 picoammeter, with a 42 volt bias voltage between the MCP and the photocathode. The quantum efficiency is calculated from the ratio of these two quantities, less the dark current in each.

The UV LED source was stepped across the LAPPD window, and at each step, the input light intensity was measured, as well as the resulting photocurrent. The map is shown in Figure 12. The maximum quantum efficiency is ~14%. The X-spacers are visible in the map. The QE is highest in the central region.

The QE spectrum is also shown in Figure 12, from a selected location near the center after the photocathode was manufactured. The highest measured sensitivity is at 365 nm.

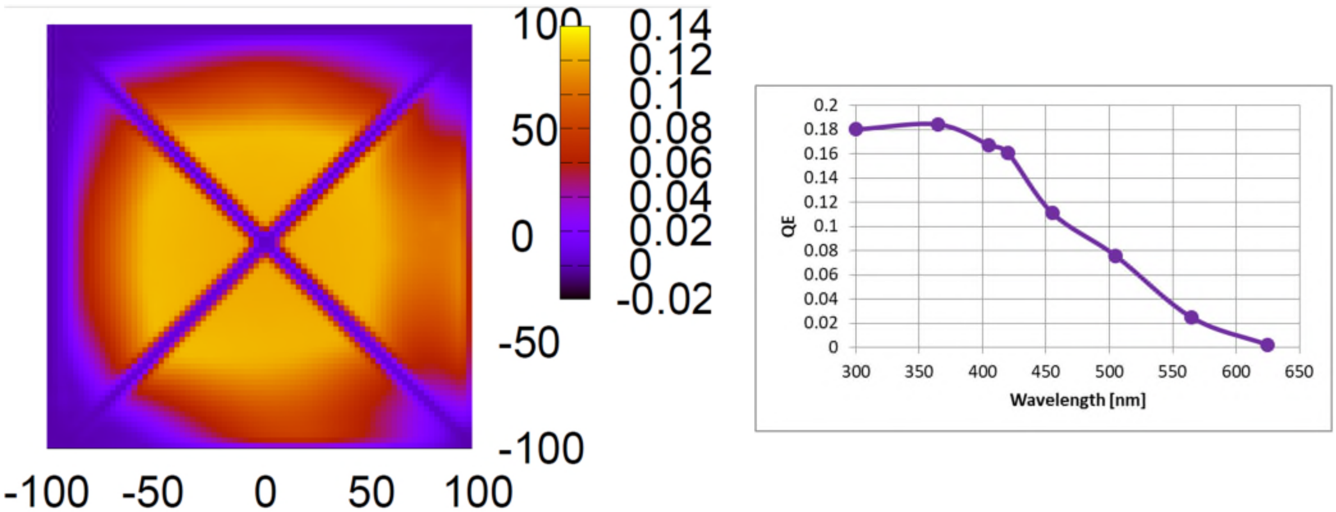

Figure 12. Left: A photocathode Quantum Efficiency map is shown at 365 nm. QE is ~14% at maximum. Right: A QE spectrum is shown at elevated temperature, following fabrication.
L:\Engineering\LAPPD-Test-Station\Photocathode scans\LAPPD 29\LAPPD 29 05-10-2018\

MCP resistance vs. voltage

The MCP resistance is shown in Figure 13, as a function of voltage. They are non-ohmic, and their resistance decreases somewhat with increasing voltage. Some of this behavior may be attributed to warming, as the MCP resistance decreases with increasing temperature. The resistive film in this pair of MCPs is quite uniform, as the MCPs do not thermally run away. The low resistance is also advantageous for high rate operation. The variation of resistance with voltage in Figure 7 must be considered if a resistor divider network will be used to distribute high voltages.

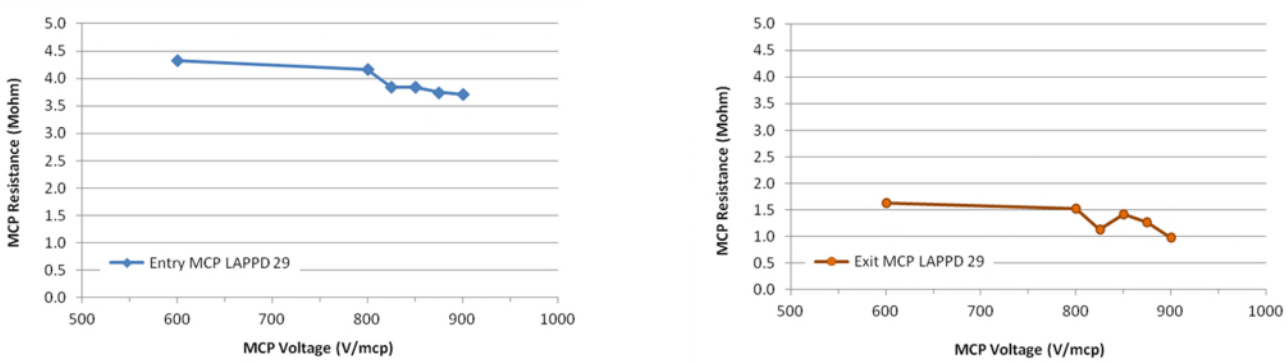

Figure 13: MCP resistances for LAPPD 29. C00101-049 is the entry MCP (left), and C00113-028 is the exit MCP (right).

High voltage connection diagram

The high voltages may be connected as shown in Figure 14 for maximum control of the LAPPD. This approach separates the current paths of the entry and exit MCPs, so anomalies in either may be detected. Additionally, the photocathode voltage may be controlled independently of the MCPs. Without changing the gain, the photocathode voltage may be increased, which will increase the gain somewhat as the photoelectrons acquire more energy before impacting the microchannel. Alternatively, it may be decreased so it is more positive than the entry side of the entry MCP. In this case, the photoelectrons will remain at the photocathode, and the MCP dark pulses may be observed. This state may also be used if an accidental exposure of the LAPPD to light is anticipated.

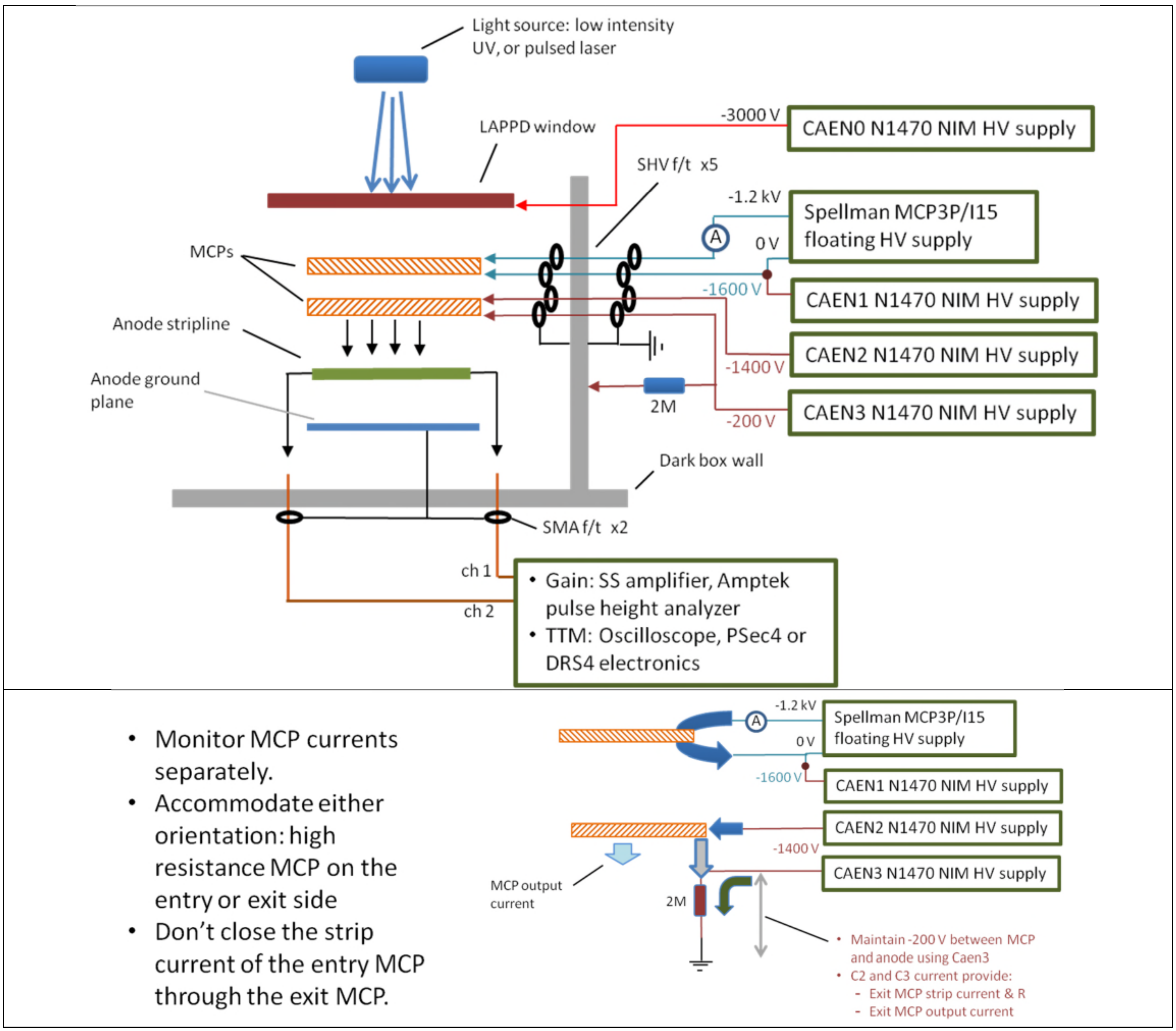

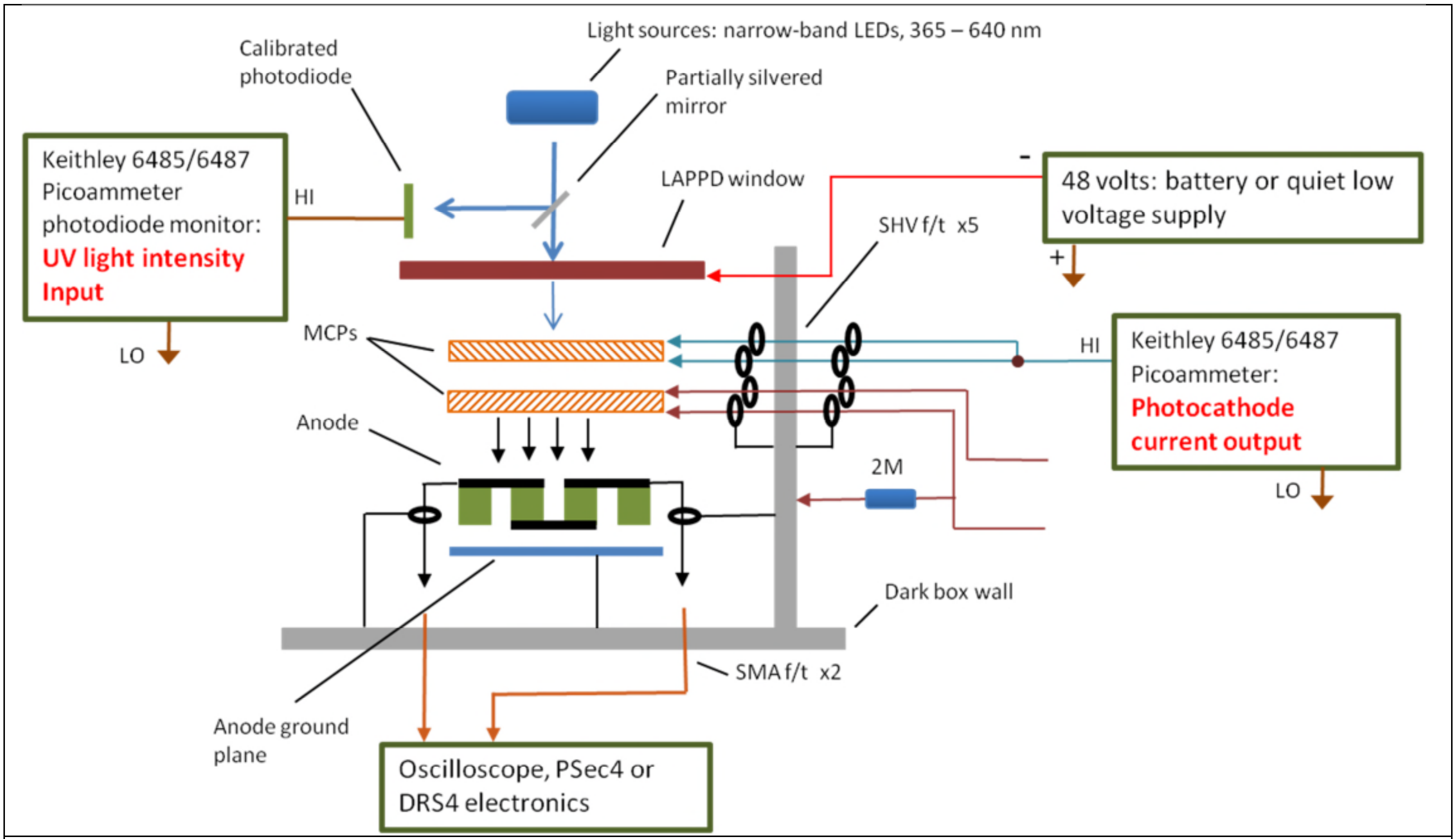

Figure 14. **Top:** The wiring diagram for high voltage and signals is shown for the LAPPD gain and timing testing at Incom. **Middle:** A schematic shows the separation of the two MCP current paths, and the techniques used to separately measure the output current to the anode and the strip current through the exit MCP. **Bottom:** The wiring diagram for the QE measurement is shown. The exit MCP and the anode are not involved in this measurement. Instead, the entry MCP serves as the anode for the photocurrent.

Connectivity

An ultem housing and a backplane are provided with each LAPPD (Figure 15). The backplane connects the strips to SMA connectors with near-50 ohm impedance. The ultem housing provides the high voltage connections. They consist of SHV panel mount connectors on the outside, and Mill-Max spring-loaded ball tip pins on the inside. The pins touch the high voltage pads on the LAPPD envelope. The 5 high voltage connectors are labeled according to their function. The shields on the SHV connectors simply terminate the high voltage cable shield, and minimize unwanted signal pickup in the detector. They do not close any high voltage current paths.

Packing

The LAPPD is wrapped in foil and placed in a Pelican case with antistatic foam (Figure 15). The foil helps manage static charging, which could be harmful to charge-sensitive electronics that will be attached to it. It also keeps unnecessary stray light from exciting the photocathode, and charging the entry MCP.

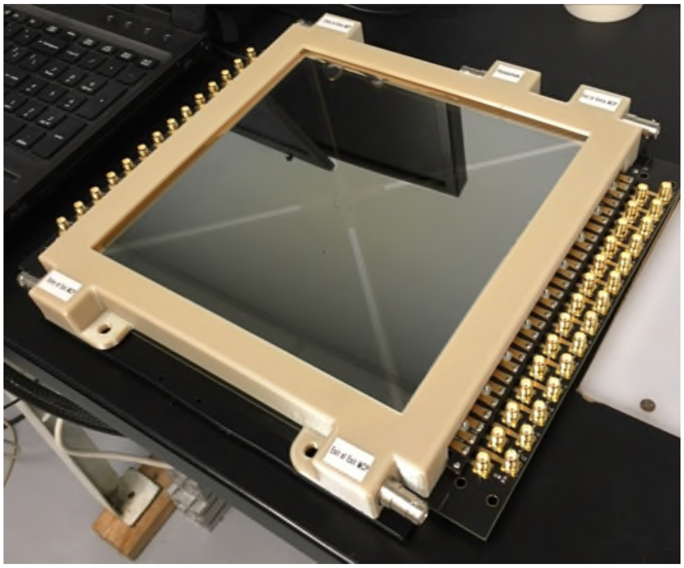

Figure 15. **Left**: the LAPPD is enclosed in a housing with high voltage connectors, and mounted on a backplane for signal access. **Right**: The LAPPD is wrapped in foil to manage static charging, and to keep stray light from the photocathode.